Thermo-Hygral Analysis on Long-Term Natural Frequency of RC Buildings with Different Dimensions

Ryota Kurihara , Nobuhiro Chijiwa , Koichi Maekawa

Journal of Advanced Concrete Technology, volume 15 (2017), pp. 381-396

Journal of Advanced Concrete Technology Vol. 15, 381-396, August 2017 / Copyright © 2017 Japan Concrete Institute

Scientific paper

Thermo-Hygral Analysis on Long-Term Natural Frequency of RC Buildings with Different Dimensions

Ryota Kurihara[1], Nobuhiro Chijiwa[2] and Koichi Maekawa[3*]

Received 19 April 2017, accepted 17 August 2017 doi:10.3151/jact.15.381

Abstract

Gradual decay of natural frequency of reinforced concrete (RC) buildings is computationally investigated in view of the long-term moisture loss and associated shrinkage of concrete. The thermo-hygral analysis for RC lifetime over several decades is applied with monitoring data of existing multi-story buildings and nuclear power plants in service. The reduced natural frequency is numerically reproduced with delayed cracking near junction planes between structural members of different dimensions in multi-story buildings and dispersed cracks close to the surfaces of RC thick walls of nuclear power plants. In order to quantitatively clarify the impact of drying shrinkage, both sealed and open boundary conditions for moisture migration are assumed at simulation. It is also confirmed logically that the rate of decay for the natural frequency of the middle story RC building is faster because of the small thickness of walls, slabs and columns compared to structural members of nuclear power plants.

1. Introduction

Volumetric change of concrete caused by moisture loss (drying) and heat liberation (hydration) has been taken into account in design of structural concrete as well as on-site construction for reducing the risk of cracking and unexpected deformation. Afterwards, structural concrete is generally exposed to ambient states and external loads. Especially, moisture loss and associated shrinkage of concrete with large dimensions is known to be in progress for a long time (Gilbert 2013) as well as the short-term performances (Gribniak *et al.* 2013).

Yoshida *et al*. (1987) investigated the effect of drying shrinkage on the initial overall stiffness of bridge piers and their inelastic seismic resistances. The nonlinear elasto-plastic finite element analysis with zero tensile strength was also recommended to simply consider the effect of cracking caused by drying shrinkage. The authors presented the predictive method for the long-term excessive deflection of large-scale PC viaducts for more than 30 years (Maekawa *et al.* 2015; Ohno *et al.* 2012; Bazant *et al.* 2010). Here, the moisture loss and associated mechanics are the key factor and considered in JSCE design code 2012 as a differential shrinkage of box-sectional viaducts.

Recently, so called health monitoring of existing structures is focused on as an effective asset management and quick judgement of safety just after earthquake's impacts (Seki *et al.* 1996). Since the overall structural stiffness which we may easily sensor by accelerometer is linked with damaging of constituent members and materials such as cracking and yielding of steel (Masi *et al.* 2010; Trifunac *et al.* 2001), monitoring data has been published for several concrete structures in the past years (Oliveira *et al.* 2010; Calvi *et al.* 2006).

The periodical structural monitoring of a nuclear power-plant building has been conducted as well and its overall natural frequency has been reported to gradually decay for 30 years (Ogata *et al.* 2011). Similar gradual decrease was also reported for a middle story concrete building (Kashima and Kitagawa 2006; Abe and Mori 2005; Toyobe *et al*. 2013). The reduced natural frequency means the reduction of global structural rigidity under the small variation of stresses and strains. On the varying natural frequency, Maruyama (2016) reported an advanced investigation of interest from a multi-scale views of material as moisture loss and stiffness change, and structural member aspect as drying shrinkage induced cracking. Both factors are pointed out as a key issue of structural management. In this paper, the authors express their full support with this view and try to quantitatively deepen the understanding in more macroscopic structural aspect.

Here, the authors' attention is directed to the different rates of reduced natural frequency throughout the lifetime. The power plants whose walls have large thickness of 1~2m exhibit their slower reduction of natural frequency than the middle story buildings do with much smaller dimensions of columns and slabs (**Fig. 1**; Maruyama 2016). In fact, the rate of moisture loss to cause drying is associated with the absolute dimensions of structural members (Samouh *et al.* 2016; Yoneda *et al.* 2015, 2013). The authors reported the drying effect on

[1]Graduate student, Department of Civil and Environmental Engineering, Tokyo Institute of Technology, Tokyo, Japan.
[2]Associate Professor, Department of Civil and Environmental Engineering, Tokyo Institute of Technology, Japan.
[3]Professor, Department of Civil Engineering, The University of Tokyo, Tokyo, Japan. *Corresponding author, *E-mail:* maekawa@concrete.t.u-tokyo.ac.jp

the dynamic responses of a multi-story RC building even under small seismic actions (**Fig. 2**; Chijiwa and Maekawa 2015). The larger floor drifts were computed as the real ones behaved by the presence of shrinkage cracks and associated stiffness decay.

The seismic response of the 28-story tower building was also observed in Chiba at March 11, 2011 of Tohoku Earthquake, Japan, and its dynamic response analysis

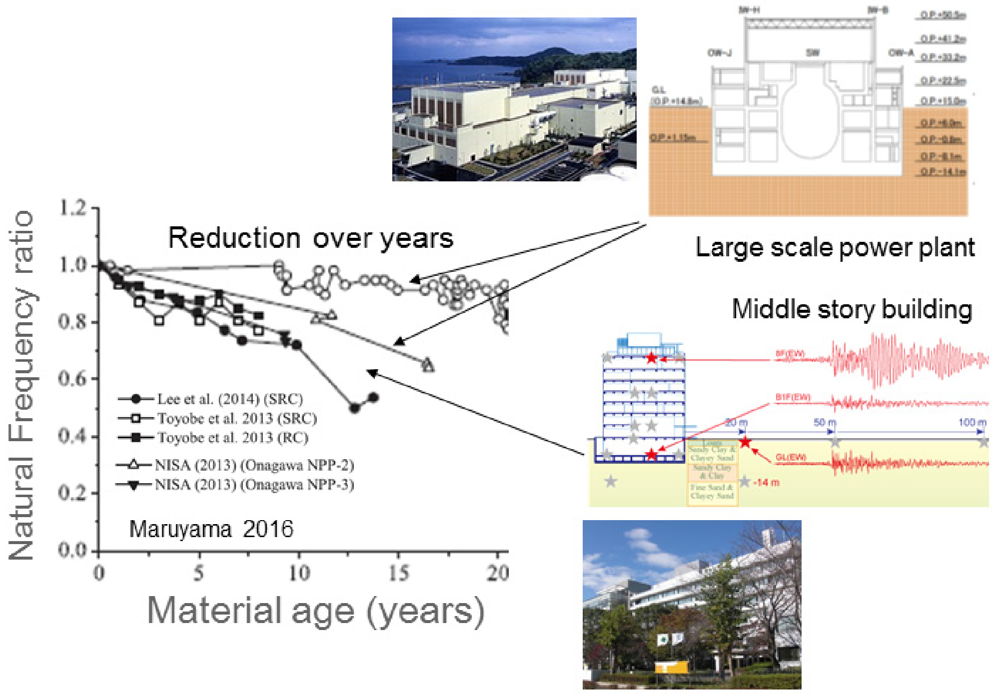

Fig. 1 Reduced natural frequency of concrete structures with different dimensions (Maruyama 2016).

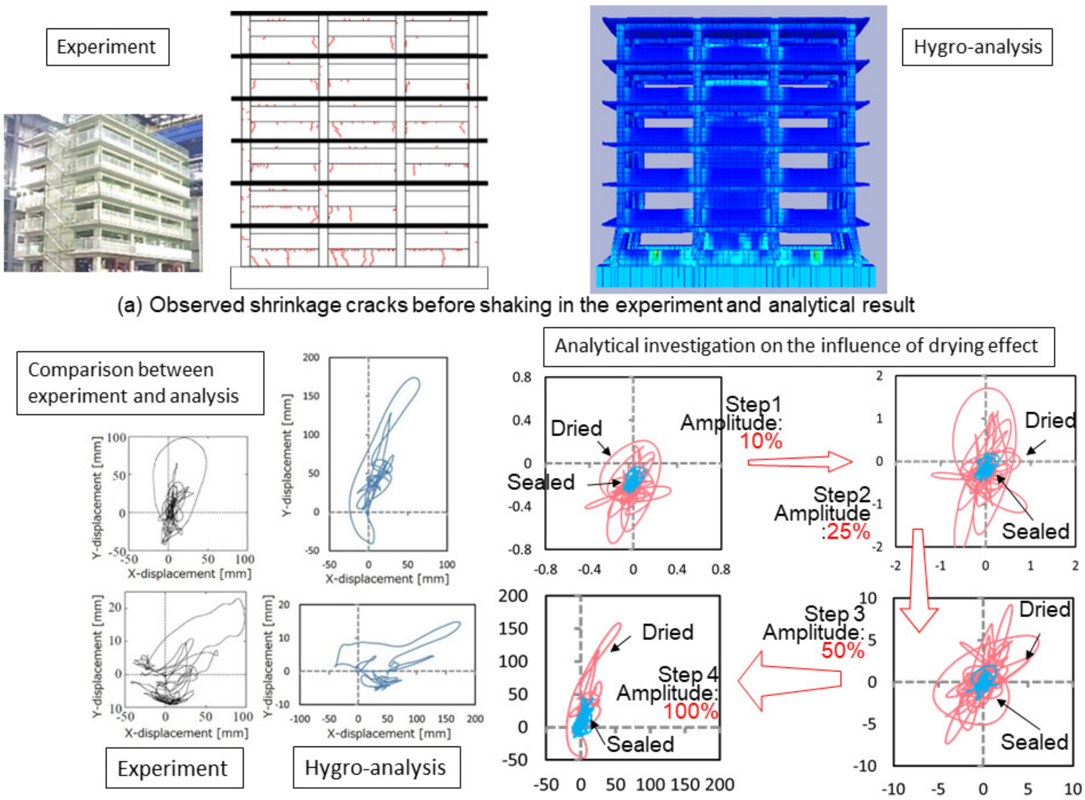

(a) Observed shrinkage cracks before shaking in the experiment and analytical result

(b) Displacement of 2nd floor in horizontal direction(X-Y) (Lateral axis: X, Vertical axis: Y, Unit: mm)

Fig. 2 Seismic response analysis of RC building with and without drying (Chijiwa and Maekawa 2016).

was conducted by Ikawa *et al.* (2012). The successful seismic responses of computation attribute to the reduced initial stiffness (about 15%) as shown in **Fig. 3**. As the ground motion in Tokyo was comparatively less enough not to jump into high inelasticity, the reduced stiffness used for the dynamic analysis is thought to be closer to the realty of the building just before the earthquake and at 18 years after construction. These facts are on structural responses against short-term mechanistic actions of small magnitude. Thus, we have possibly almost no irrecoverable event like yield of steel and cracking of concrete.

On the contrary for higher permanent loads like underground ducts, the authors reported the inelastic irrecoverable events which is accelerated by moisture loss and finally may lead to delayed out-of-plane shear failure for several decades after construction (Maekawa *et al.* 2016).

The objective of this study is to numerically investigate the scale effect on the variation of structural initial rigidity and the natural frequency over decades, and the source of its transient variation is focused in view of cracking and deformational mode of structures (Rots 2001; Giardina *et al.* 2010). Then, simplified in discussion are other effects such as construction quality, temperature, static interaction with soil foundation (Bindi *et al.* 2015; Trifunac *et al.* 2001), properties of cement, admixture agents and construction processes. Then, the authors expect that the monitored natural frequency of buildings and infrastructures may play an important role as a reference on which the damage assessment of structural concrete under heavy loading can be based (Meshke *et al.* 1999; Belleri *et al.* 2014; Hyun *et al.* 2003; Kumari and Kwatra 2013).

2. Multi-Scale Thermo-Hygral Analysis

For discussing the scale effect on the structural stiffness with different dimensions, the simulation of moisture transport and related shrinkage, self-equilibrated stresses, crack nonlinearity and mode of deformation shall be taken into account (Grasberger and Meschke 2004; Maekawa *et al.* 2003; Meschke *et al.* 1999). The effect of sustained stresses as long-term actions must be considered as well (Asamoto *et al*. 2008; Castel *et al*. 2013). Then, the authors apply the multi-scale thermo-hygral analysis (Maekawa *et al.* 2008, 2003; Yoneda *et al.* 2013, 2015) for both multi-story RC buildings and large-scale power plants as shown in **Fig. 4**. Here, the solidification constitutive modeling of concrete is used for hygro-mechanical coupling (Ishida *et al.* 1998; Mabrouk *et al.* 1998).

In the past, this system was applied by Chijiwa and Maekawa (2015) to simulate the nonlinear dynamics of the real scale mockup of 6-story RC building (Matsumori *et al.* 2008) on the shaking table as shown in **Fig. 2**. The hygral effects of moisture were concluded to be crucial for inelastic dynamic responses of small and middle magnitudes as well as linear elasticity in motion. Then, the authors select the same building for the first discussion and comparison, because inelastic dynamic responses as well as the initial stiffness were precisely recorded and the real-scale mockup's detail was clearly known including the construction processes. Then, the detailed explanation of the real-scale building experiment is given to the reference (Matsumori *et al.* 2008).

In the analyses, joint interface elements between members were not placed for simplicity, but cracking which develops in elements close to neighboring members with different shapes and dimensions numerically represents the kinetics of junction. As this crack is the indirect and week expression of localized junction planes with small sized finite elements, the multiplication of shear strain and the element size is mechanically equivalent to the shear slip of the junction plane. Then, the shear transfer model of RC elements results in the model of junction planes. We have the same story for the mode of tension normal to the joint planes.

2.1 Multi-story RC building

In order to focus on the drying effect alone, firstly, one-time casting of fresh concrete is numerically as-

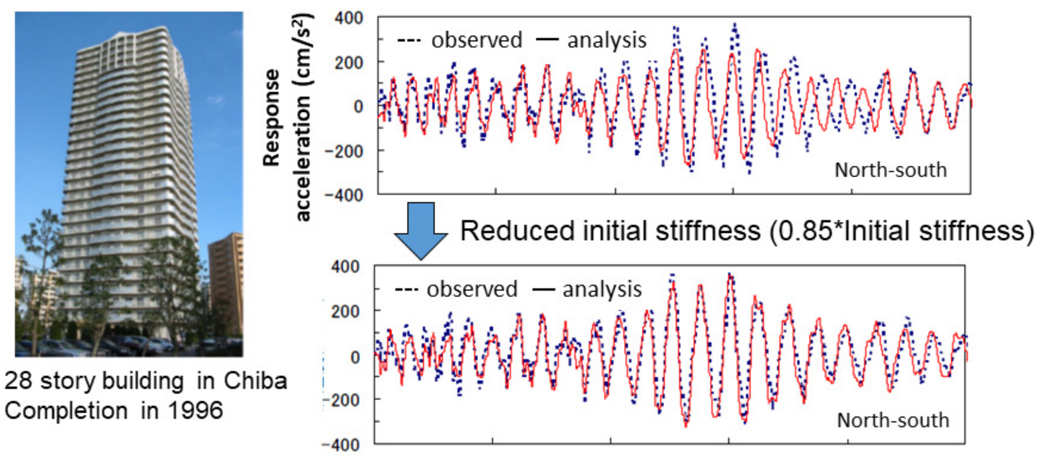

Fig. 3 Seismic analysis of 28-story RC building with reduced initial stiffness (Ikawa *et al.* 2012).

Table 1 Mix proportion of concrete used for Multi-story RC building analysis.

W: water (kg/m^3)	C: cement (kg/m^3)	W/C (%)	G: gravel (kg/m^3)	S: sand (kg/m^3)	Air (%)
160	290	55	1000	850	4.0

Note) Specific gravity: normal Portland cement=3.15, gravel=2.58, sand=2.65.

sumed to make a simultaneous start of cement hydration and micro-pore formation at all finite elements under zero gravity (Chijiwa and Maekawa 2015). During this period of initial hydration, perfect sealed conditions were set up. After 7-days curing, the whole structure was exposed to 60% relative humidity (RH) and the vertical gravity of 980 gal. The mix proportion of concrete simulated is listed in **Table 1**. As the mockup was constructed on the shaking table inside the laboratory, no effect of rain fall is considered. At each elapsed time, the horizontal gravity of 10 gal, i.e., constant equivalent static force proportional to the mass of concrete, was fictitiously applied for a few minutes and the horizontal drift of each floor was computed. Thus, the averaged shear stiffness of each story was calculated.

When the cracking is newly introduced in plain concrete without reinforcement, the sudden change of stiffness occurs and is easily observed in reality. But, in the case of normal reinforced concrete with steel embedded, the averaged stiffness reduction gets mild owing to the steel's stiffness and the presence of bond. Thus, the experimentally obtained tension stiffness curves exhibit almost smooth reduction of averaged tensile stiffness even though the crack evolution still proceeds (Maekawa *et al*. 2003, Vecchio and Collins 1986). This is unlike the case of tension softening of plain concrete as well. Then, smooth trend of the overall structural stiffness reduction is thought to be reasonable and it is hard to identify the crack occurrence only with the global response of entire structures.

Figure 5 shows the computed variation of the averaged horizontal rigidity of the entire structural concrete. If the perfect sealing would be continued for the whole lifetime, the stiffness gradually increases according to the progressive hydration of cement, following pore-structure formation and development of material stiffness (Maekawa *et al.* 2003). Thus, the overall stiffness comes up to the maximum at about 200 days.

On the contrary, the overall structural stiffness is gradually declining if drying and moisture loss are numerically allowed. In order to clarify the sensitivity of key factors, aggregate shrinkage is not numerically con-

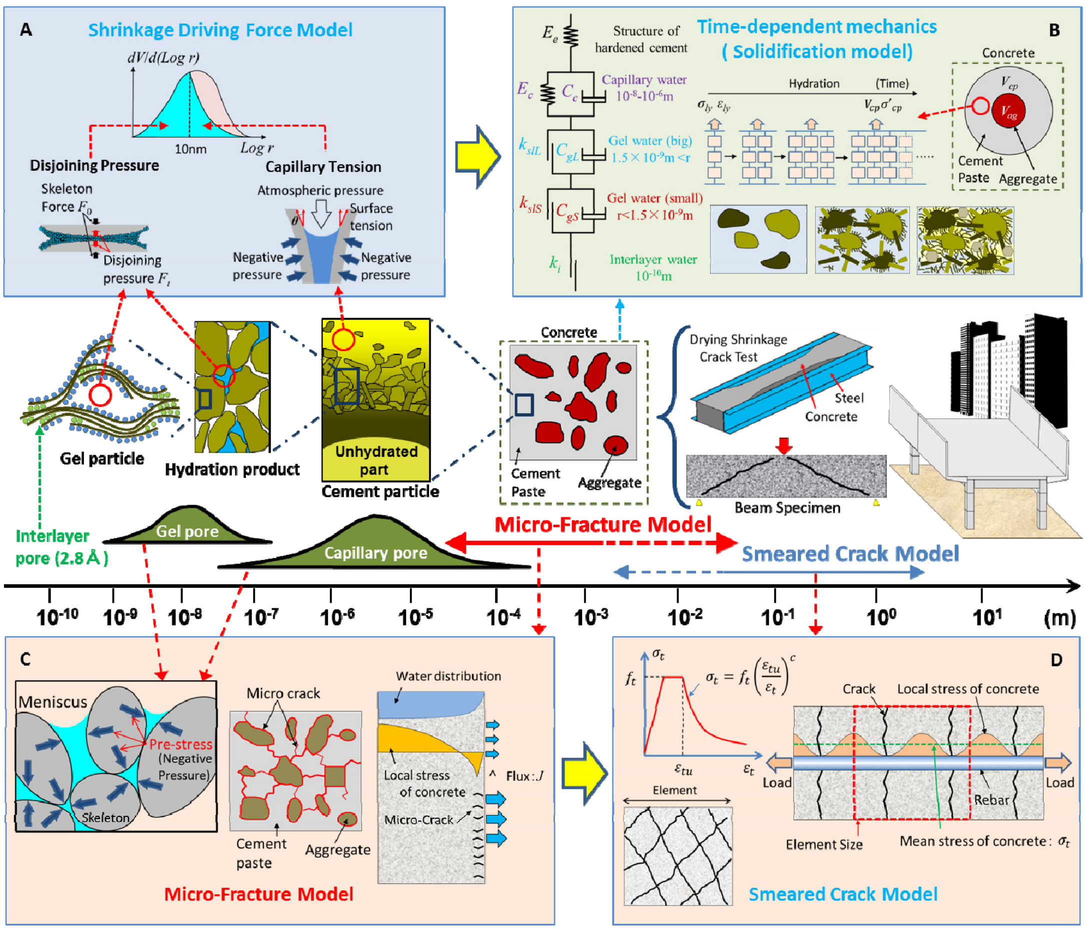

Fig. 4 Schematic platform of multi-scale thermo-hygral analysis (Yoneda *et al.* 2013, 2015).

Table 2 Mix proportion of concrete used for thermo-hygral analysis of nuclear power plant.

W: water (kg/m^3)	C: cement (kg/m^3)	W/C (%)	G: gravel (kg/m^3)	S: sand (kg/m^3)	Air (%)
175	325	54	946	802	5.0

Note) Specific gravity: normal Portland cement=3.16, gravel=2.58, sand=2.62.

sidered but surface tension of water in capillary pores and disjoining pressure in gel pores in cement paste alone (Imamoto and Arai 2008; Asamoto *et al.* 2008; Goto and Fujiwara 1979) are taken into account. The global stiffness is taken in the X-direction as shown in **Fig. 5**. The stiffness at 50 years is simulated to drop to about 50% of the initial one at 7 days. This is equivalent to about 70-60% of the natural frequency as discussed later. This is close to the case of the 28-story RC building shown in **Fig. 3**. As the reference age on which the building stiffness reduction is based was not reported, we cannot have strict comparison with the analysis where the referential age is 7 days. But, if the referential age of the analysis would be set forth at 28 days, the apparent computed shear stiffness reduction becomes about 20%. Thus, it may be possible to say that there is a similar trend. In this case, the development of material stiffness is also hindered numerically because of the premature cement hydration owing to the loss of water at the early ages.

The mode of deformation of the drying case is shown in **Fig. 5**. The in-plane shrinkage of each floor introduces the flexure of columns with flexural cracking at the column-slab connections of the first floor. As walls and columns with different specific surface area are sparsely arranged on each floor, out-of-plane distortion of each floor can be seen owing to differential shrinkage among members. Consequently, cracking of concrete is concentrated mainly at the junction between different members. The macroscopic effect by cracking is not negligible as well as the retarded micro-pore structure development due to water loss. This coupled micro and macro mechanism will be further investigated in later chapters.

2.2 Nuclear power plant model

As stated in **Chapter 1**, nuclear power plants exhibit the gradual reduction of the natural frequency (Ogata *et al.* 2011). Basically, buildings containing reactors in Japan consist of strong walls so that they possess high stiffness which results in short period of vibration and greater capacity against large seismic actions. Then, the dimension of walls is about 1.0~2.0m by thickness and the specific loss of moisture per volume must be thermodynamically less compared to normal RC building.

Figure 6 shows the finite element discretization for the thermo-hygro analysis (Maekawa *et al.* 2003). The target structure's dimension and shape are plainly decided in reference to power plants (Ogata *et al.* 2011). As RC walls are designed to function against in-plane shear with distributed cracking, reinforcement of all walls is arranged to be smeared out and its ratio by volume is set forth as 1.2% in both horizontal and vertical directions, respectively. For the base slab, orthogonal reinforcement of 1.0% is assumed as well.

The mix proportion of concrete simulated is listed in **Table 2** so that the computed compressive strength of concrete may get close to that of the material test of 34MPa at 28 days. In fact, the varying strength and stiffness of concrete are calculated step by step based upon the developed micro-pore structures in simulation. We arrange two cases. One is no aggregate shrinkage (Goto and Fujiwara 1979), and computationally shows about 350 micro shrinkage of the standard specimen (Yoneda *et al.* 2015). The other one specifies 0.04% of

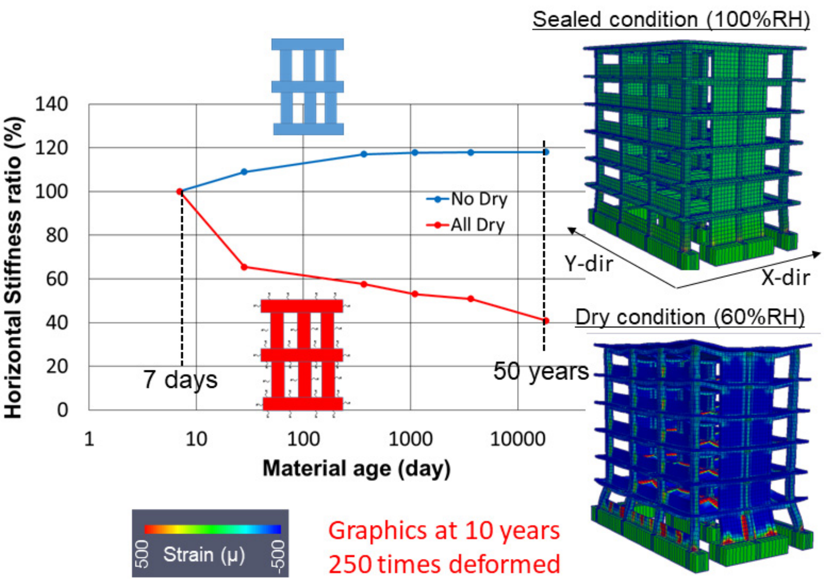

Fig. 5 Averaged drift stiffness of the whole structures.

the maximum capacity of intrinsic aggregate shrinkage which brings about 900 micro shrinkage (Asamoto *et al.* 2008; Imamoto *et al.* 2006, 2005; Fujiwara 1984). The intrinsic shrinkage capacity of aggregates used has become the primary factor for shrinkage of concrete composites in recent years in Japan, although it was practically governed by the unit water content.

For discussing the scale effect, the small model with 1/20 dimension is also prepared with the same material and the reinforcement ratio as shown in **Fig. 6**. Thus, the dimension of members is about 10cm by thickness, which is similar to the case of RC building as shown in **Fig. 5**. The coupling of scale effect (macro-view) and the specific shrinkage of concrete (meso-view) are underlined.

The computational curing and the exposure to the ambient conditions are the same as those of the case of RC building (**Fig. 5**). In order to avoid the impact of thermal stresses, the nodal temperature was fixed to be 20 degree Celsius. Then, pure coupling of moisture loss and the structural stiffness can be discussed in this section. The computed structural stiffness normalized by the value at 7 days after casting is shown in **Fig. 7**. Here, the overall structural rigidity is the totally applied static horizontal force divided by the horizontal displacement at the center of the top floor slab.

As the thickness of walls is more than 1.0m, the rate of moisture loss normalized by volume is much less at the beginning of drying. Even after the exposure to the natural environments, water loss from concrete accompanying the retardation of cement hydration is concentrated only nearby the surfaces. Then, the strength gain continue to evolve for large volume of core concrete, and the overall structural stiffness is increasing up to almost 200 days. After this period, the gradual decline of the global stiffness in X-direction can be seen in **Fig. 7** similar to the case of RC building. This reduction does not converge but continues for more than 30 years as the real case is (Ogata *et al.* 2011), and we have the stability around 50 years when the thermo-hygral equilibrium with the natural environment holds computationally.

The shrinkage develops more uniformly over the walls and the strain near the junction planes looks less localized unlike the case of multi-story RC building. Then, let us focus on the single wall component. The same curing is applied to a single RC wall with 2m thickness and the in-plane stiffness of the wall is computed as shown in **Fig.**

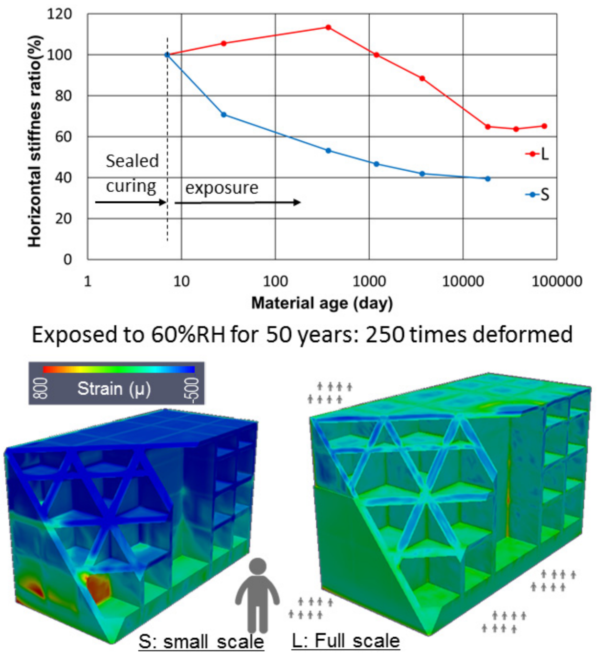

Fig. 7 Transient structural stiffness of power plant under small variation of stress and strain.

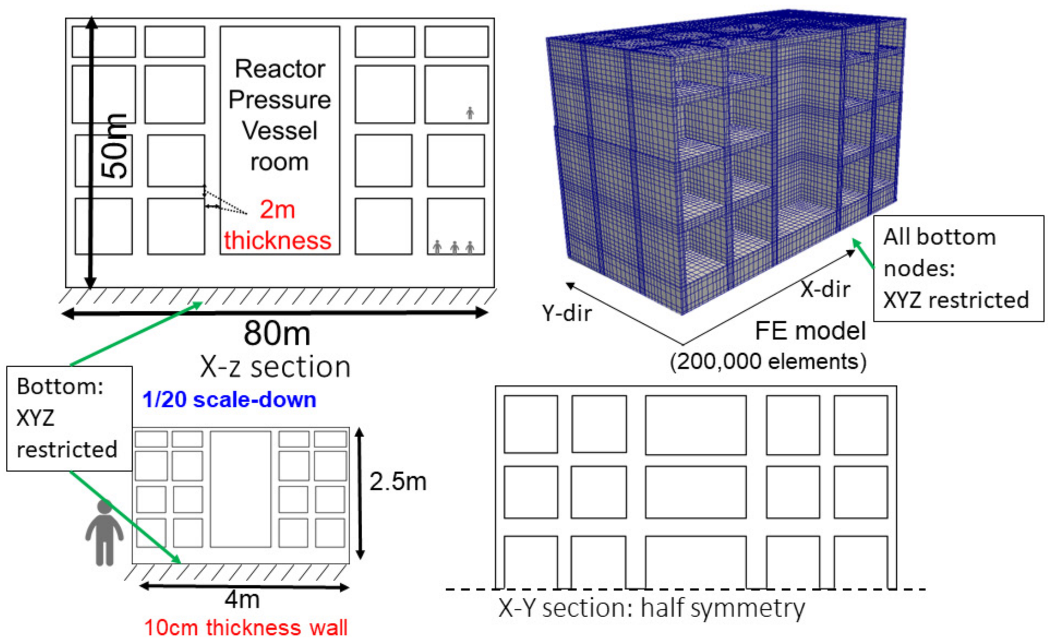

Fig. 6 Real scale mockup model of nuclear power plant and its scale down.

8. Moisture migrates normal to the 2D extent of the wall and drying shrinkage proceeds from the surface layer to the core center. Four corners are firmly restrained for 1 and 50 years. Afterwards, the short-term shear deformation is introduced and the shear reaction is obtained. The reduction rate of the rigidity of the single wall are similar to that of the entire structures. In fact, nuclear power plant buildings are designed as an assembly of in-plane walls. Then, the source of the entire structural stiffness decay under the small stress and strain states is chiefly rooted in the transient decay of wall's stiffness.

Although the initial stiffness of the wall is greatly influenced by shrinkage, the nonlinear restoring force characteristics is less affected as shown in **Fig. 8**. The shear capacity is mainly governed by the yield of bi-directional reinforcement. Even though the shrinkage of concrete is introduced for long time of 50 years, overall ductility is not substantially changed. As a matter of fact, design values of ductility and the skeleton curve of shear walls were specified several decades ago in reference to laboratory tests whose mechanism was affected by drying shrinkage owing to thin thickness of about 10-20cm.

The simulation of the scale-down mockup of 1/20 brings about the contrast of interest as shown in **Fig. 7**. The gain of structural rigidity after 7 days cannot be seen, because the impact of moisture loss is greater than the case of large size and the solidification cannot come up to the full capacity due to shortage of water during the cement hydration in concrete. The different deformation modes can be seen at the same age of structures. The shrinkage of the upper part of the small structure arises widely and uniformly, and the lower part is well confined by the base slab. Thus, the seismic performance of the plants is thought not to be degraded.

But, for the large structure, the shrinkage is rather localized around the surfaces of slabs and walls, because the drying does not completely reach the core of thick members. As the thickness of walls of upper floors is smaller than those of lower floors, we have a small amount of effect of moisture loss from the lower story. Similar to the case of RC building's mockup in **Section 2.1**, the strain is rather localized at the extreme ends along the peripheral lines. It implies that the cracking introduced nearby junction planes of members may chiefly weaken the overall rigidity of the whole structural system.

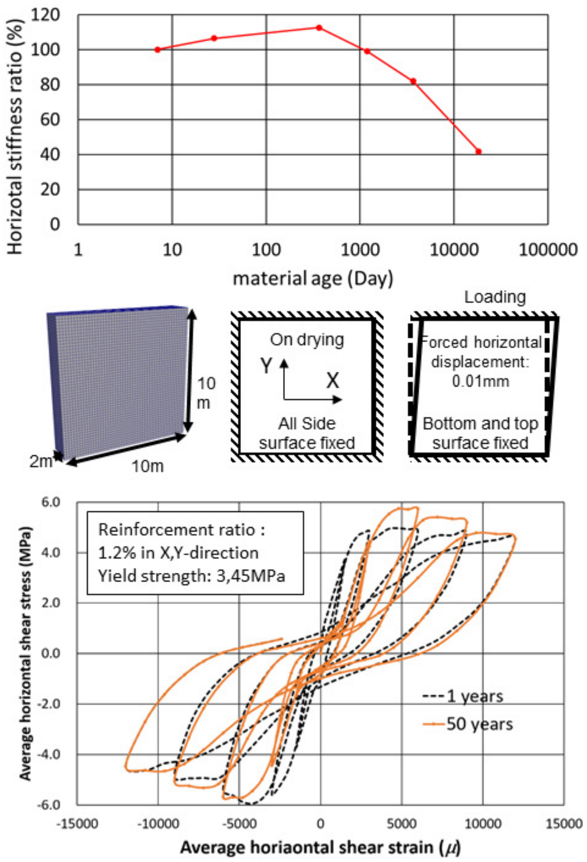

Fig. 8 Effect of shrinkage on the initial stiffness and the restoring force characteristics.

2.3 Scale dependent reduction of natural frequency of structural concrete

The overall stiffness of the whole structural concrete under the small variation of stresses and strains can be converted to the natural frequency from the structural rigidity by simply assuming the piecewise linear one-degree of freedom lumped mass system, that is to say, the natural frequency of the first mode free vibration is proportional to the square root of the stiffness (Abe and Mori 2005). In order to check the conversion, after the equivalent static input of the small gravity in the horizontal direction, this force was suddenly released and obtained the natural vibration, and both values were verified to coincide with each other.

As shown in **Fig. 9**, slow decay of the natural frequency is simulated for the large RC power plant facilities and multi-story buildings. The prediction is not so far from the reality of monitoring at site. In order to capture the whole range of lifetime, the logarithmic scale of time is also chosen, and the computed frequency is normalized by the value at the age of 28 days for RC buildings and one year for nuclear plants after construction. The decay of natural frequency continues over 30 years. In case of the record of ONAGAWA-#1 (records from 1985 to 2010), we can see the reduction of stiffness just after the earthquake of smaller magnitude, but a quick recovery was also accompanied. In fact, the decay of stiffness by the earthquake is comparatively less than that of the computed reduction by shrinkage. Then, the reduction of building stiffness is thought to mainly attribute to the thermo-hygral effect.

On the other hand, the record of ONAGAWA-#2, #3 (records from 1995 to 2011), which includes the damage by the Tohoku Great Earthquake on March 11th, 2011, shows substantial reduction of stiffness just after the quake and the stiffness decay seems to be accelerated similar to the case of high aggregate shrinkage. Then, it can be said that there are some multiple causes of stiffness reduction for a long time of service, and the drying shrinkage impact cannot be avoided for the investigation of long-term global building stiffness. Here, the authors want to point out the cross-effect of mechanistic and thermo-hygral actions as well. When the cracking is introduced by the mechanical actions, the rate of drying is known to be accelerated afterwards (Bazant *et al.* 1987), because the cracking can be a short-cut path of vapor migration. This cross-effect is also taken into account in the thermo-hygral analysis used in this study (Yoneda *et al.* 2015). The authors hope to leave this multiple impact in this study as the future topic of deeper investigation.

The decreasing rate of the natural frequency looks similar for both RC buildings of normal size and power plants of large scale. But, it must be noted again that the referential ages are different for both structures as stated above. For large-scale nuclear reactors, their overall stiffness rises for about three years as shown in **Fig. 7**. But at this time, the RC multi-story building's stiffness has been already down as shown in **Fig. 5**. Thus, the absolute stiffness decay and associated natural frequency are much size-dependent.

It should be also noted that these analyses do not completely imitate the reality of existing RC. We use simple assumption for structural shapes and dimensions, and the typical material properties of concrete and reinforcement were assumed. The arrangement of reinforcing bars does not match real individual nuclear plant building, but the normal use was referred. For clear discussion on scale effect alone, the authors intentionally avoid the effect of thermal stresses.

It is known in these days that concrete shrinkage is much affected by the aggregate shrinkage (**section 2.2**). Its influence on the power plants of large section and the multi-story building of the middle section is described in **Fig. 9.** The wider variation of the natural frequency can be seen in both cases. It may be attributed to the quality of aggregates used in view of the intrinsic shrinkage (**Appendix**). Thus, quality of aggregate is thought to be influential for middle to large-scale structural concrete as well as smaller ones.

It is hard to have a universal conclusion only with these sensitivity analyses discussion. But, within the limited information, the authors may conclude at least that the moisture loss and associated structural cracking may play some substantial role on the decay of natural frequency of structural concrete owing to both cracking (macro) and hydration degree (micro aspect), and that the coupled consideration of the hygral and mechanistic issues is critical for the scale effect of natural frequency decay. In order to deepen our understanding of the decay of structural rigidity and the harmonic vibration frequency, the authors conduct some sensitivity analyses from a viewpoint of meso-scale in between micro and macro.

3. Sensitivity Analysis on Meso-Scale

Decay of the natural frequency of the entire structure is caused by micro and macro factors. Thus, the sensitivity

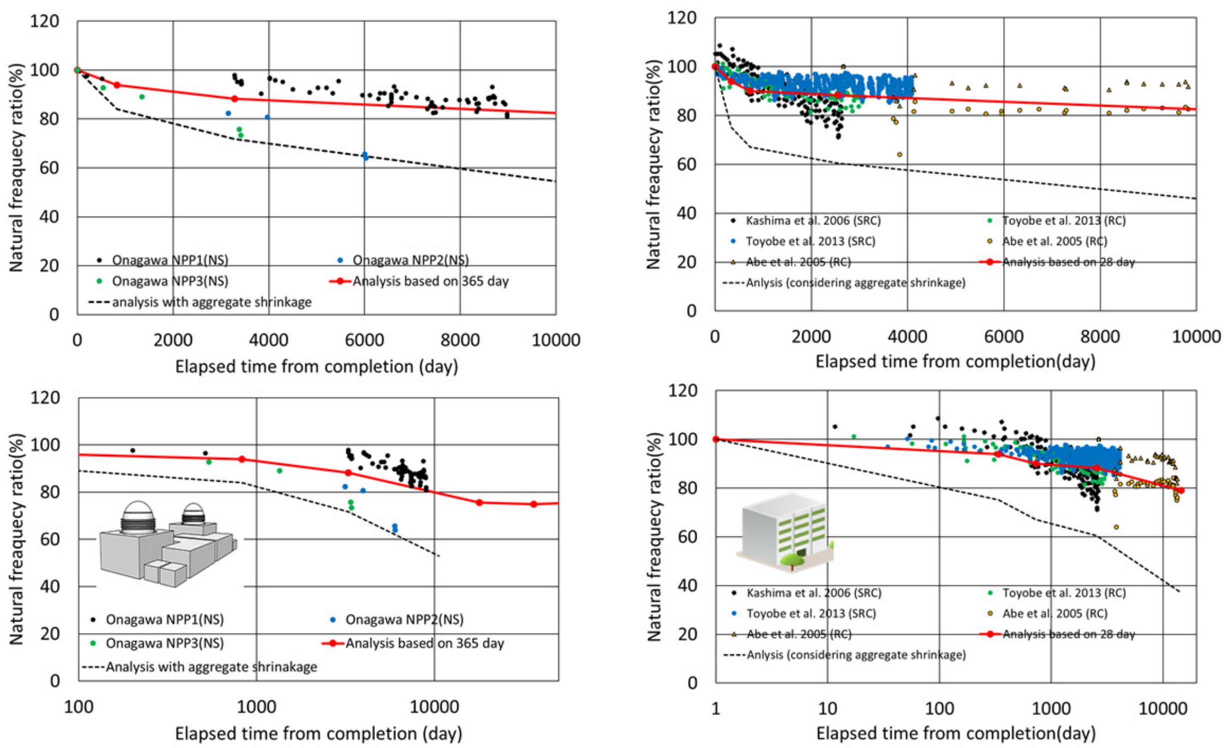

Fig. 9 Computed transient natural frequency over the life time of RC structures with largely different dimensions: left=nuclear plant, right=multi-story building.

analysis with different local ambient conditions around each member may be beneficial for more deep insight into the mechanism. Here, three types of boundary conditions are intentionally defined as shown in **Fig. 10**. The standard case is that all structural members are exposed to dry air of 60% RH. Another is the case where only slabs are exposed to drying and other columns and walls are under sealed conditions, and vice versa.

Beforehand, the effect of curing period on the overall stiffness was examined. **Figure 10** shows the case of 28 days sealed curing. Just before the exposure, the cement hydration proceeds and the strength development and the associated stiffness evolved. The following decay of rigidity is similar to the case of 7 days curing as the reference. Then, the following discussion is made based on the 7 days sealed curing case.

After the building is exposed to air, cracks are formed mainly around the junction planes and their surroundings as shown in **Fig. 2** at the middle of drying. In the experiment, shrinkage cracks were also observed at the walls confined by slabs or columns before dynamic loading (Matsumori *et al.* 2008), and the computed result coincides with the fact. Cracking in junction planes is hardly observed in general, and there is no close-up report at junction planes between members. Thus, it is the point of observation and monitoring of real-scale structural concrete in future to clarify the discussion.

The shrinkage of slabs brings about local deformation of corner columns on the first floor like necking. But, the columns and walls of the upper floors are not so much deformed. In fact, the decay of the horizontal rigidity is mild compared to other cases. The mere shrinkage of columns and walls, which are the main resistant mechanism against the floor drift, contrarily introduces much self-equilibrated stresses and cracking, and rapid reduction of the whole structural rigidity as shown in **Fig. 10**. This deformational mode attributes to the non-uniform arrangement of axial stiffness of interior columns and sparsely arranged shear walls. The members arranged at core center are tightly confined by the floors rather than the exterior columns and walls. Here, in all cases, the base part is firmly fixed to the foundation and no substantial deformation is produced.

Figure 11 shows the variation of shear stiffness normalized by the value at 7 days when the drying begins numerically. The shear stiffness of each story can be calculated by the relative horizontal displacement of a pair of adjacent floors divided by the static shear force

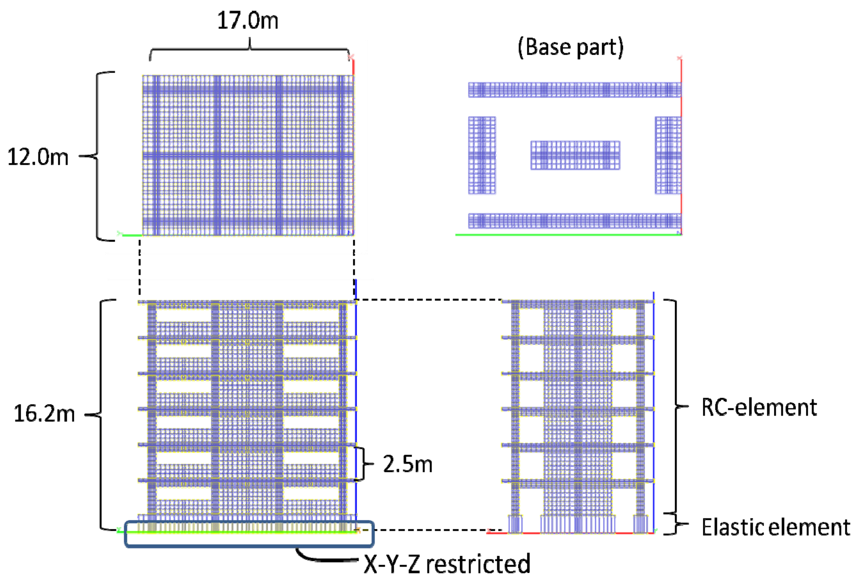

(a) Finite element discretization and member arrangement (Chijiwa and Maekawa 2016).

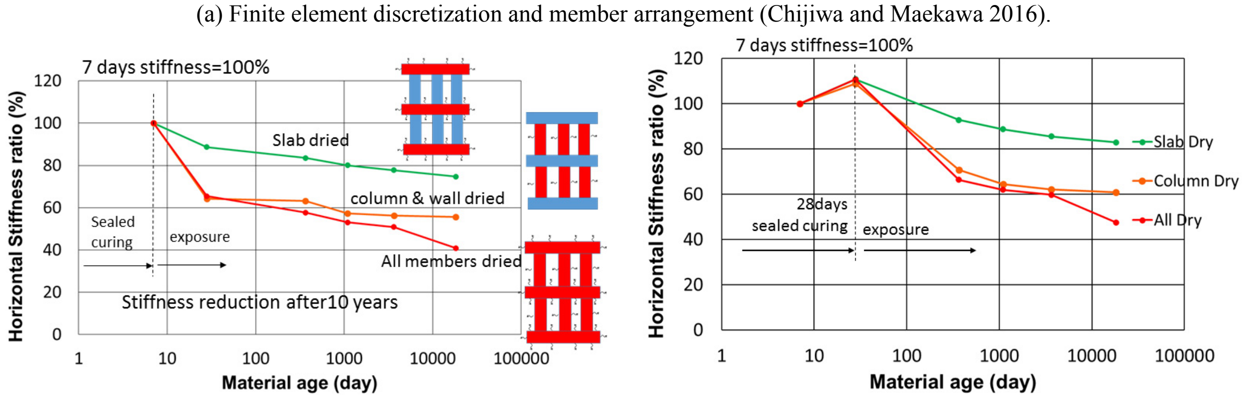

(b) Horizontal stiffness decay of each local drying condition.

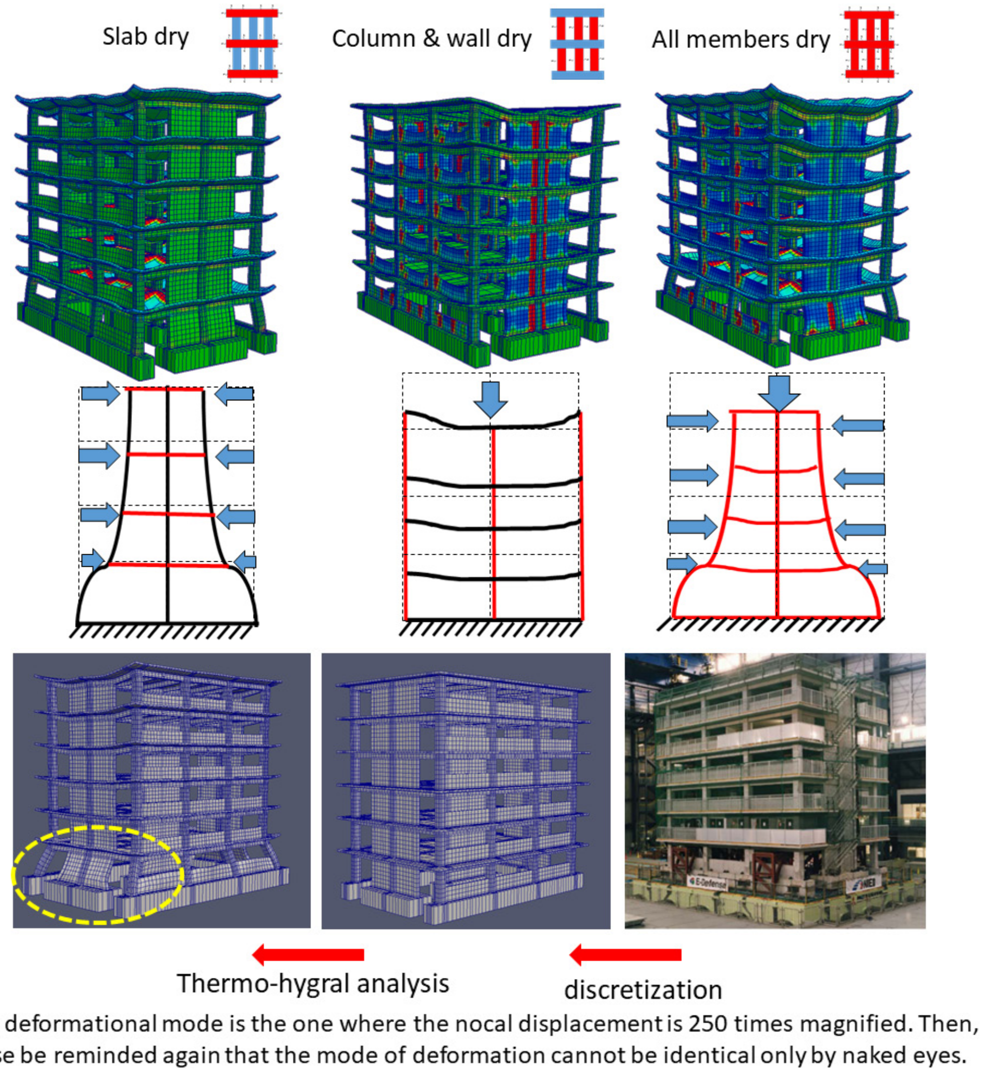

(c) Deformational mode of each local drying conditions.

Fig. 10 Effect of partial drying shrinkage on the overall stiffness.

applied to each floor. In the case of dried slabs, the averaged stiffness of each story is kept less changed over the lifetime. This is consistent with the results in **Fig. 10** although the localized necking is produced to the columns on the first floor.

The case of dried columns & walls causes larger reduction of the shear stiffness of all stories. RC columns have some shrinkage cracking at the surface zone due to moisture loss and flexural stiffness is declined. Furthermore, the volumetric change of shear walls is greater due to large specific surface area. Drying of all members are similar to the case of column & wall shrinkage without no moisture loss of other members. Then, it can be concluded that the shear stiffness reduction and transient decay of the natural frequency derive chiefly from macroscopic structural mode of deformation and structurally induced cracking.

In order to confirm the impact of shrinking floor slabs, the horizontal nodal restraint of the bottom layer of the base part is released as shown in **Fig. 12** (denoted by no confinement). Since the base part is horizontally liberated, the necking to the RC column at the first floor almost disappears compared to the upper floors. Then, the self-equilibrated stresses by floor's volumetric change are confirmed to be a major factor of the structural stiffness reduction and its transient decay. **Figure 12** shows the closed up of the strain profiles of columns and walls around the first floor. The concentrated deformation arises nearby the junction planes between the base part and the attached structural members.

The gravity action (dead weight) introduces the axial forces to columns. Then, the flexural stiffness gets a bit larger since the opening of the flexural cracks is imprisoned and the permanent compression may hold back the shrinkage cracking. But as shown in **Fig. 13**, even if the gravity action gets lost fictitiously, the horizontal stiffness decay is almost the same as that of the normal case. Needless to say, the axial compressive force is not the key factor.

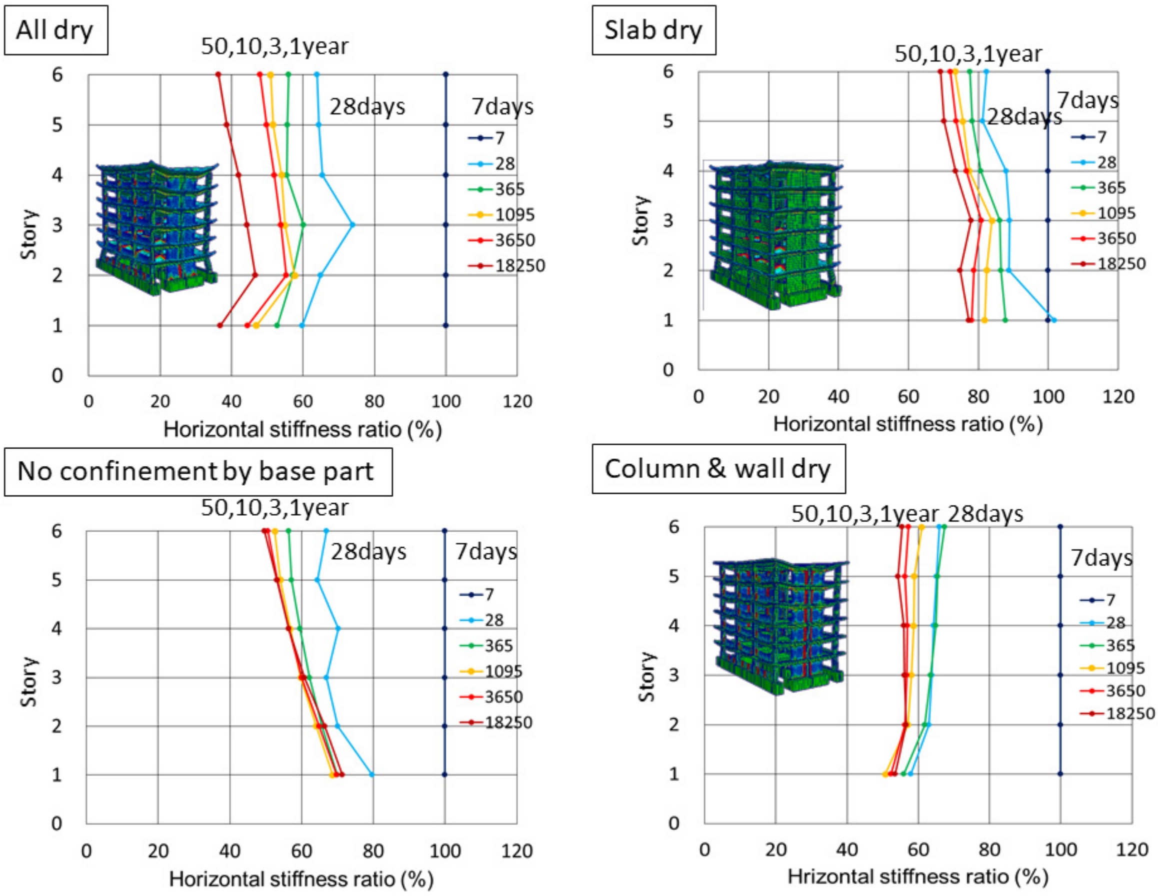

Fig. 11 Effect of partial drying shrinkage on the overall stiffness.

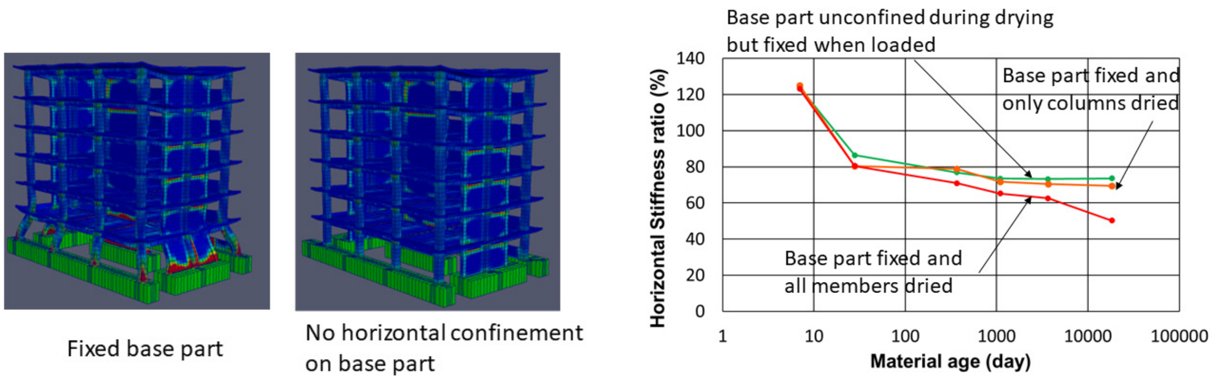

Fig. 12 Base part confinement to the columns on the first floor.

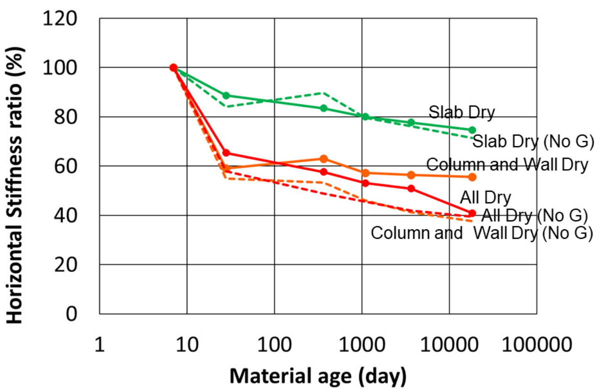

Fig. 13 Stiffness decay under zero gravity.

4. Conclusion

The drying shrinkage of concrete is a key factor to predict the overall stiffness and associated natural frequency of the whole buildings of different dimensions, and the size of structural members is confirmed to be a critical factor of moisture loss and associated volume changes. Then, the multi-scale hygral analysis was employed to simulate the lifetime variation of the natural frequency and the following conclusions were earned as,

1) The varying shear stiffness of each floor of the multi-story building is mainly governed by the states of drying of columns and shear walls. The shrinkage of floors induces the self-equilibrated deformation to the columns of the first floor but its impact is not primary.
2) A mockup model of RC power plant buildings is also affected by the moisture loss and associated shrinkage although its dimension is almost 10 times greater than the one of normal RC building, but the rate of decay of natural frequency is slower, and it can be quantitatively explained by the coupling analysis of moisture migration and the nonlinear mechanics with cracking.
3) The shrinkage effect may chiefly come to the junction planes between members of different dimensions especially for the case of normal RC buildings. Structural cracking is the main source of stiffness decay. Here, it is numerically confirmed that constituent members have no deterioration of their functions as a structural unit against the external actions.
4) As a matter of course, the seismic responses of the buildings are affected by the shrinkage under the ground motions, and it was numerically confirmed.
5) The natural frequency and the vibration mode of real individual building depend on several factors although the drying is thought to be one of common factors of importance. Thus, it will be necessary to consider the stiffness decay of moisture effect as a base line when the impact of earthquake is to be estimated just after the great event.

The stiffness reduction and the decay of vibration frequency of buildings and power plants are caused by at least multiple factors. It must be said that the overall rating of probable cause of them cannot be quantitatively identified by this study. Though systematic parametric sensitivity analyses and large-scale mock-up, however, the authors raise the point that moisture migration and associated volume change of concrete can be one of unavoidable factors to be discussed quantitatively. For further investigation, we may need monitoring data and systematic inspections of real buildings and infrastructures in line with the stock management.

Acknowledgements

The authors express their gratitude to Dr. Zhu of Shimizu Corporation and Dr. Nakarai of Hiroshima University for their suggestions and discussions. This research is financially supported by MEXT/JSPS KAKENHI 23226011.

References

Abe, Y. and Mori, K., (2005). "Research study on degradation of natural frequency of reinforced concrete buildings by micro tremor measurement." *Prep. Architectural Institute of Japan Tohoku Branch*, Structure (68), 89-92.

Asamoto, S., Ishida, T. and Maekawa, K., (2006). "Time-dependent constitutive model of solidifying concrete based on thermodynamic state of moisture in fine pores." *Journal of Advanced Concrete Technology*, 4(2), 301-323.

Asamoto, S., Ishida, T. and Maekawa, K., (2008). "Investigations into volumetric stability of aggregates and shrinkage of concrete as a composite." *Journal of Advanced Concrete Technology*, 6(1), 77-90.

Bazant, Z. P., Yu, Q., Li, G. H., Klein, G. and Kristek, V., (2010). "Excessive deflections of record-span prestressed box girder." *Concrete International*, 32(6), 44-52

Bazant, Z. P., Sener, S. and Kim, J. K., (1987). "Effect of cracking on drying permeability and diffusivity of concrete." *ACI Materials Journal*, 84 (Sept.-Oct.), 351-357.

Belleri, A., Moaveni, B. and Restrepo, J. I., (2014). "Damage assessment through structural identification of a three-story large-scale precast concrete structure." *Earthquake Engineering & Structural Dynamics*, 43(1), 1-158.

Bindi, D., Petrovic, B., Karapetrou, S., Manakou, M., Boxberger, T., Raptakis, D., Pitilakis, K. D. and Parolai, S., (2015). "Seismic response of an 8-story RC-building from ambient vibration analysis." *Bulletin of Earthquake Engineering*, 13(7), 2095-2120.

Calvi, G. M., Pinho, R. and Crowley, H., (2006). "State-of-the-knowledge on the period elongation of RC buildings during strong ground shaking." *First European Conference on Earthquake Engineering and Seismology*, Grneva.

Castel, A., Gilbert, R. I. and Ranzi, G., (2013). "Overall stiffness reduction of cracked reinforced concrete beams due to long term effects." *Ninth International Conference on Creep, Shrinkage, and Durability Mechanics* (CONCREEP-9), 443-450.

Chijiwa, N. and Maekawa, K., (2015). "Thermo-hygral case-study on full scale RC building under corrosive environment and seismic actions." *Journal of Advanced Concrete Technology*, 13(10), 465-478.

El-Kashif, K. F. and Maekawa, K., (2004). "Time-dependent nonlinearity of compression softening in concrete." *Journal of Advanced Concrete Technology*, 2(2), 233-247.

Fujiwara, T., (1984). "Change in length of aggregates due to drying." *Bulletin of the International Association of Engineering Geology,* 30(1), 225-227.

Gilbert, R. I., (2013). "Time-dependent stiffness of cracked reinforced and composite concrete slabs." *Procedia Engineering*, 57, 19-34.

Giardina, G., Hendriks, M. and Rots, J. G., (2010). "Numerical analysis of tunneling effects on masonry buildings: the influence of tunnel location on damage assessment." *Advanced Materials Research*, Vol.133-134, 289-294.

Grasberger, S. and Meschke, G., (2004). "Thermo-hygro-mechanical degradation of concrete: From coupled 3D material modelling to durability oriented multi-field structural analyses." *Materials and Structures,* 37, 244-256.

Gribniak, V., Kaklauskas, G., Kliukas, R. and Jakubovskis, R., (2013). "Shrinkage effect on short-term deformation behavior of reinforced concrete - When it should not be neglected." *Materials & Design*, 51, 1060-1070.

Goto, Y. and Fujiwara, T., (1979). "Effect of aggregate on drying shrinkage of concrete." *Journal of JSCE,* 286, 125-137.

Hyun, C. H., Koh, H. M., Cho, H. H., Lee, S. K. and Choi, K. R., (2003). "Development of seismic damage assessment system for nuclear power plant structures in Korea." *Transactions of the 17th International Conference on Structural Mechanics in Reactor Technology* (SMiRT 17), Prague.

Ikawa, N., Fujii, A., Ito, S. and Furuki, T., (2012). "Evaluation of earthquake response of high-rise building during the 2011 off the Pacific Coast of Tohoku Earthquake." *Konoike Construction Co. Ltd. Technical Report*.

Imamoto, K. and Arai, M., (2008). "Simplified evaluation of shrinking aggregate based on BET surface area using water vapor." *Journal of Advanced Concrete Technology*, 6(1), 69-75.

Imamoto, K., Ishii, S., and Arai, M., (2006). "Drying shrinkage properties of concretes with several kinds of aggregate and the influence of specific surface areas of the aggregates." *Journal of Structural and Construction Engineering, Architectural Institute of Japan*, 606, 9-14.

Imamoto, K. and Arai, M., (2005). "The influence of specific surface area of coarse aggregate on drying shrinkage of concrete." *Creep and Shrinkage and Durability Mechanics of Concrete and Other Quasi-brittle Materials* (Concreep.7), Nantes, 95-100.

Ishida, T., Chaube, R. P., Kishi. T. and Maekawa, K., (1998). "Micro-physical approach to coupled autogenous and drying shrinkage of concrete." In: E. Tazawa Ed. *Autogenous Shrinkage of Concrete* Japan Concrete Institute, E & FN Spon.

Kashima, T. and Kitagawa, Y., (2006). "Dynamic characteristics of a building estimated from strong motion records using evolution strategy." *Journal of Structural and Construction Engineering*, 602, 145-152.

Kumari, B. and Kwatra, N., (2013). "Finite element modeling of a multi-storeyed retrofitted reinforced concrete frame." *IOSR Journal of Mechanical and Civil Engineering* (IOSR-JMCE), 8(3), 8-22.

Mabrouk, R. T., Ishida, T. and Maekawa, K., (1998). "Solidification model of hardening concrete composite for predicting autogenous and drying shrinkage." In: E. Tazawa Ed. *Autogenous Shrinkage of Concrete,* Japan Concrete Institute, E & FN Spon.

Maekawa, K., Zhu, X., Chijiwa, N. and Tanabe, S., (2016). "Mechanism of long-term excessive deformation and delayed shear failure of underground RC box culverts." *Journal of Advanced Concrete Technology*, 14(5), 183-204.

Maekawa, K., Ishida, T., Chijiwa, N. and Fujiyama, C., (2015). "Multiscale coupled-hygro mechanistic approach to the life-cycle performance assessment of structural concrete." *Journal of Materials in Civil Engineering,* ASCE, 27(2), A4014003, 1-9.

Maekawa, K., Ishida, T. and Kishi, T., (2003). "Multi-scale modeling of concrete performance -Integrated material and structural mechanics (invited)." *Journal of Advanced Concrete Technology*, 1(2), 91-126.

Maruyama, I., (2016). "Multi-scale review for possible mechanisms of natural frequency change of reinforced concrete structures under an ordinary drying condition." *Journal of Advanced Concrete Technology*, 14(11), 691-705.

Masi, A. and Vona, M., (2010). "Experimental and numerical evaluation of the fundamental period of undamaged and damaged RC framed buildings." *Bulletin of Earthquake Engineering*, 8(3), 643-656.

Matsumori, T., Kabeyazawa, T., Shirai, K. and Igarashi, K., (2008). "Shaking table test on a full-scale, six-story R/C building structure." Special project for earthquake disasters mitigation in urban areas in 2005, improvement of seismic performance of structures by E-Defense, *Technical Note of the National Research Institute for Earth Science and Disaster Prevention*, No.321.

Meschke, G., Huemer, Th. and Mang, H. A., (1999). "Computer-aided retrofitting of a damaged RC cooling tower shell." *Journal of Structural Engineering*, 125(3), 328-337.

Ogata, Y., Hirotani, K., Aizawa, N., Inoue, N. and Nozawa, T., (2011). "A study of initial stiffness on the building changed by passing age at small and medium-sized earthquake motion by ARX model." *Summaries of technical papers of annual meeting*, AIJ, B-2, Structure II, 983-984.

Ohno, M., Chijiwa, N., Suryanto, B. and Maekawa, K., (2012). "An investigation into the long-term excessive deflection of PC viaducts by using 3D multi-scale integrated analysis." *Journal of Advanced Concrete Technology*, 10(2), 47-58.

Oliveira, C. S. and Navarro, M., (2010). "Fundamental periods of vibration of RC buildings in Portugal from in-situ experimental and numerical techniques." *Bulletin of Earthquake Engineering*, 8(3), 609-642.

Rots, J. G., (2001). "The role of structural modelling in preserving Amsterdam architectural city heritage." In: P. B. Lourenço, P. Roca (Eds.), *Historical Constructions,* Guimarães, Portugal, 685-696.
Samouh, H., Soive, A., Rozière, E. and Loukili, A., (2016). "Experimental and numerical study of size effect on long term drying behavior of concrete: influence of drying depth." *Materials and Structures*, 49, 4029-4048.
Seki, M., Mizutani, K., Nishimura, A. and Nakano, S., (1996). "Characteristic vibration of rigid frame bridges damaged by the Hyogo-ken-Nanbu Earthquake." *Journal of JSCE*, V-33(550), 145-154.
Toyobe, R., Kojima, H., Tobita, H. and Fukuwa, N., (2013). "Long-term seismic response observation for evaluation of dynamic properties of low and midium-rise building." *AIJ Tokai Branch*, 51, 177-180.
Trifunac, M. D., Ivanović, S. S. and Todorovska, M. I., (2001). "Apparent periods of a building. II: Time-frequency analysis." *Journal of Structural Engineering*, ASCE, 127(5), 527-537.
Vecchio, F. J. and Collins, M. P., (1986). "The modified compression-field theory for reinforced concrete elements subjected to shear." *ACI Journal*, 83(2), 219-231.
Yoneda, T., Ishida, T., Maekawa, K., Gebreyouhannes, E. and Mishima, T., (2015). "A micro-cracking model coupled with micro fracture and water status in micro pore structures." *Journal of Japan Society of Civil Engineers*, Ser. E2 (Materials and Concrete Structures), 71(3), 263-282.
Yoneda, T., Ishida, T., Maekawa, K., Gebreyouhannes, E. and Mishima, T. (2013). "Simulation of early-age cracking due to drying shrinkage based on a multi-scale constitutive model." *Poromechanics V*: ASCE, 579-588.
Yoshida, I., Kanemitsu, H., Yamashita, M. and Higuchi, K., (1987). "Seismic analysis of RC pier with earthquake resistant wall." *Journal of JSCE*, I-8(386), 349-358.

Appendix

1) Drying shrinkage strain of representative members for each structure.

In the hygral analysis used, volumetric shrinkage of concrete is associated with the moisture migration analysis and driving force of capillary tension and disjoining pressure (Yoneda *et al*. 2015). Then, the rate of shrinkage is different according to the geometry of structural concrete. For example, **Fig. A1** shows the FE discretization and corresponding averaged shrinkage strain (60% RH after 7 days of form strip) of the standard specimen. Concrete mix proportion used in the analysis is listed in **Table A1**. The shrinkage strain is not the input value of the analysis but the computed value under the specified exposure conditions.

2) Governing Equation for moisture migration.

The mass conservation of moisture transport used in this study is expressed as (Maekawa *et al*. 2008),

$$\frac{\partial \theta}{\partial t} + div\left(J(\theta, \nabla\theta)\right) + Q = 0 \qquad \text{(A1)}$$

where, θ [kg/m^3] is the mass of water in a unit volume of concrete, t [s] is the time, J [kg/m^2·s] is the moisture flux and Q [kg/m^3·s] is the sink term related to cement hydration. Thus, we have the flux term of Eq. (A1) as,

$$J = -(D_p \nabla P_l + D_T \nabla T) \qquad \text{(A2)}$$

where, D_p [kg/Pa·m·s] is the combined moisture conductivity with respect to the pore pressure denoted by P_l [Pa] and D_T [kg/K·m·s] is the moisture conductivity with respect to the temperature T [K]. During the water absorption process, the variation of temperature was controlled to be minimal in this study. Then, the right term of Eq. (A2) is negligible. Here, D_p is composed of two parts as,

$$D_p = K_l + K_v \qquad \text{(A3)}$$

where, K_l [kg/Pa·m·s] is the unsaturated liquid permeability and K_v [kg/Pa·m·s] is the vapor one.

These values are not constant but variables with respect to capillary and gel micro-pore structures and the degree of saturation (Maekawa *et a*l. 2008). For example, K_l and K_v are computed at the surface and core center of the specimen without intrinsic aggregate shrinkage as listed in **Table A1**. These values are different according to the location with different saturation degree of capillary and gel pores denoted by S_{cap} and S_{gel}. The moisture conductivity was computed to be almost unchanged up to 4 years.

Table A1 Varying moisture conductivity at 28 days.

Location	K_l [kg/Pa·m·s]	K_v [kg/Pa·m·s]	S_{cap} (porosity)	S_{gel} (porosity)	RH (%)
Surface	$2.2*10^{-17}$	$3.1*10^{-17}$	0.25 (0.26)	1.0 (0.10)	85.8
Core center	$2.7*10^{-15}$	$3.2*10^{-18}$	0.93 (0.22)	1.0 (0.10)	98.8

Note) Porosity of each pores is defined as volume fraction of concrete composite.
Note) RH: relative humidity inside the micro-pores.

3) Creep coefficients.

The time-dependent strain of concrete is computed based upon the solidification modeling linked with the micro-pore formation and moisture in pores of various sizes as shown in **Fig. 4** (Asamoto *et al*. 2007, Yoneda *et al*. 2015). Then, similar to the drying shrinkage, creep is not the input characteristics but computed value under the sustained stress states. **Figure A2** shows the computed averaged strain of the specimen under the sustained compression which was applied at 28 days under the sealed conditions. The apparent drying creep can be also simulated by changing the boundary conditions of moistures (Asamoto *et al*. 2006).

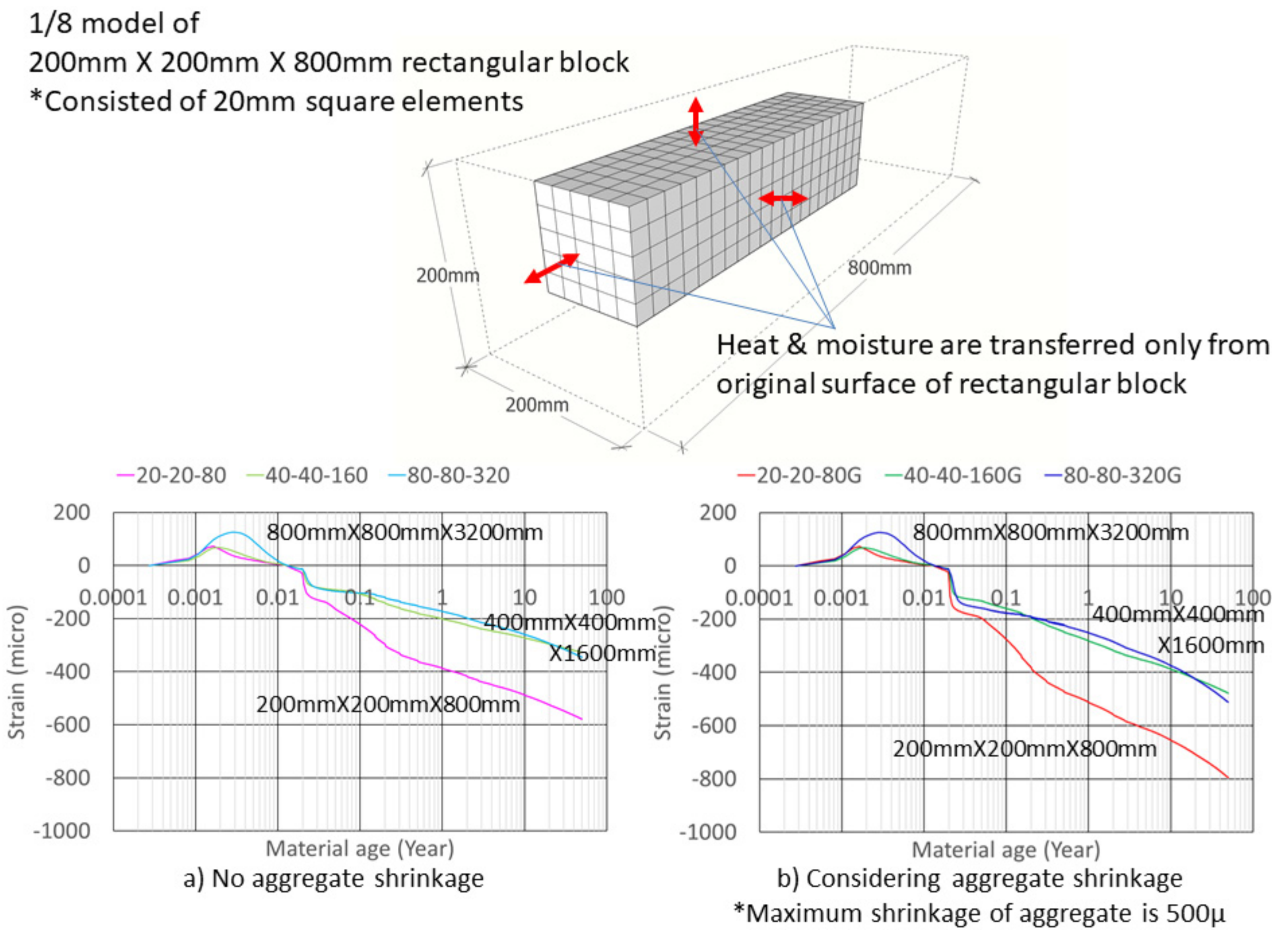

Fig. A1 Simulated drying shrinkage of the concrete specimen by thermo-hygral analysis.

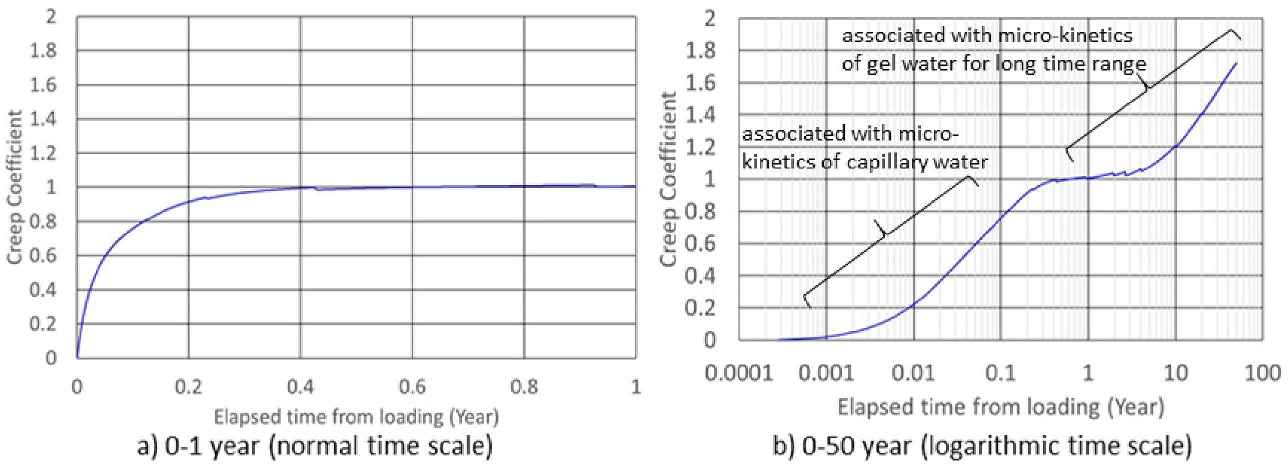

* Graph a) is a part of Graph b), and it focuses the data until 1000 days after loading

Fig. A2 Computed basic creep coefficients by thermo-hygral analysis.

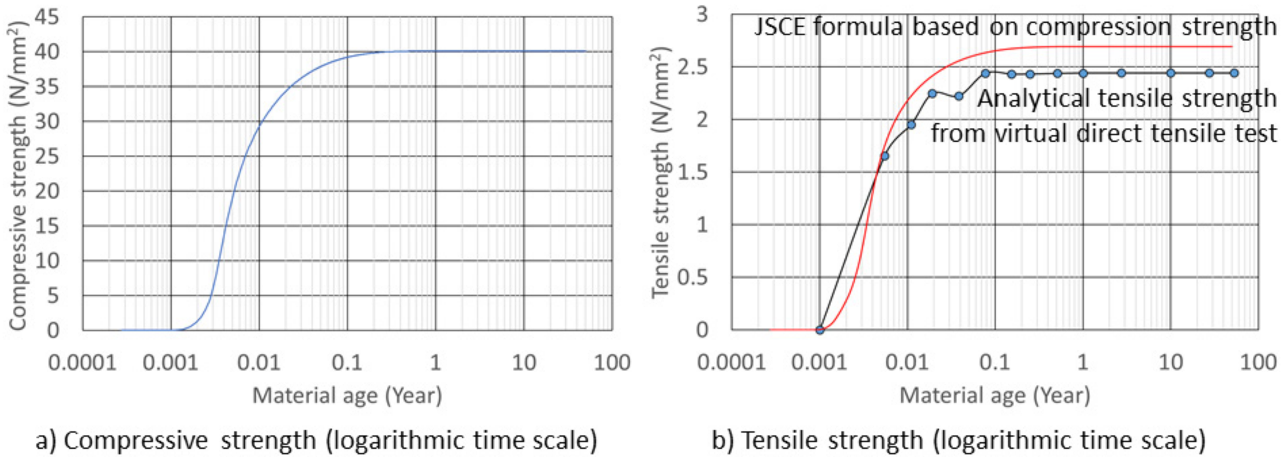

Fig. A3 Computed strength development by thermo-hygral analysis.

4) Strength development.

Similar to creep and shrinkage characteristics of concrete, strength of concrete is computed based upon the micro-pore structure formation, moisture states and time-dependent fracturing which may evolve under higher stresses (El-Kashif and Maekawa 2004). **Fig. A3** shows the computed compressive and tensile strength of the specimen as shown in **Fig. A1** under the sealed condition.